Thermoanalytical, Spectroscopic, and Morphological Study of Poly(ethylene glycol)/Poly(2-acrylamido-2-methylpropanesulfonic acid-*co*-*N*-isopropylacrylamide) Semi-Interpenetrating Network Gels

Chi Zhang, Allan J. Easteal

Department of Chemistry and Centre for Advanced Composite Materials, University of Auckland, Auckland, New Zealand

Received 30 August 2006; accepted 9 November 2006
DOI 10.1002/app.25812
Published online in Wiley InterScience (www.interscience.wiley.com).

ABSTRACT: Novel poly(ethylene glycol)/poly(2-acrylamido-2-methylpropanesulfonic acid-*co*-*N*-isopropylacrylamide) semi-interpenetrating network gels were synthesized with free-radical initiation at 70°C and characterized with differential scanning calorimetry, Fourier transform infrared and X-ray photoelectron spectroscopy, X-ray diffraction, and scanning electron microscopy. The first thermal decomposition peaks for semi-interpenetrating network gels with various proportions of 2-acrylamido-2-methylpropanesulfonic acid and *N*-isopropylacrylamide were in the range of 278–289°C, whereas for poly(2-acrylamido-2-methylpropanesulfonic acid-*co*-*N*-isopropylacrylamide) copolymer gels with corresponding proportions of the comonomers, decomposition began at about 203°C. A significant proportion of the amide groups in the semi-interpenetrating network gels with a high proportion of 2-acrylamido-2-methylpropanesulfonic acid were found to be protonated as a result of the relatively strong acid strength of 2-acrylamido-2-methylpropanesulfonic acid. The surface morphology of the dried gels varied with the relative proportions of the comonomers and was significantly different for the semi-interpenetrating network gels and corresponding copolymer gels. Strong hydrophobic and hydrogen-bonding interactions between poly(ethylene glycol) with an average molecular weight of approximately 6000 g/mol and the copolymer network were responsible for different thermal behaviors of the poly(2-acrylamido-2-methylpropanesulfonic acid-*co*-*N*-isopropylacrylamide) copolymer gels and the semi-interpenetrating network gels. © 2007 Wiley Periodicals, Inc. J Appl Polym Sci 104: 1723–1731, 2007

Key words: ESCA/XPS; hydrogels; interpenetrating networks (IPN); thermal properties

INTRODUCTION

The homopolymer of *N*-isopropylacrylamide (NIPA) is water-soluble and thermoresponsive in a readily accessible temperature range because of a lower critical solution temperature (LCST) of approximately 32°C,[1,2] which can be modified by copolymerization[3,4] and grafting[5,6] with other monomers. 2-Acrylamido-2-methyl-1-propanesulfonic acid (AMPS) is a relatively strong acid[7] that has a wide variety of applications (as itself or its salt or as a comonomer), including packaging films,[8] foam stabilizers,[9] photographic materials,[10–20] and water absorbents.[21,22] As comonomers, AMPS and NIPA have reactivity ratios of 0.24 and 1.12, respectively, so they have a relatively strong tendency for the formation of alternating copolymers.[23] Copolymerization in an aqueous solution in the presence of a crosslinker, *N*,*N*′-methylene bisacrylamide (MBAA), and poly(ethylene glycol) (PEG) leads to a semi-interpenetrating network in which PEG chains are physically combined with poly(2-acrylamido-2-methylpropanesulfonic acid-*co*-*N*-isopropylacrylamide) [poly(AMPS-*co*-NIPA)] gel.[24,25] In this work, we report experiments designed to provide a more detailed characterization of the PEG/poly(AMPS-*co*-NIPA) semi-interpenetrating network gel (SIPN) system than has been available. The only other published work that is directly relevant to these systems is by Melekaslan and Okay[26] on the swelling behavior of polyelectrolyte hydrogels in PEG solutions.

Correspondence to: A. J. Easteal (aj.easteal@auckland.ac.nz).

Journal of Applied Polymer Science, Vol. 104, 1723–1731 (2007)

EXPERIMENTAL

Poly(ethylene glycol) with an average molecular weight of approximately 6000 g/mol (PEG6000) was supplied by BDH Chemicals (Poole, UK). NIPA (Acros Organics, Geel, Belgium) and AMPS (Merck, Darmstadt, Germany) were both synthesis-grade (>99%) materials. MBAA (Sigma, St. Louis, MO) was an electrophoresis-reagent-grade material. Ammonium persulfate (APS; Ajax Chemicals, Sydney, Australia), used as an initiator, was >98% pure. All these materials were used without further purification.

Pregel solutions were made with various AMPS/NIPA molar ratios by the dissolution of appropriate

TABLE I
FTIR Spectral Bands and Assignments for PEG6000

ν (cm^{-1})	Assignment
3448	O—H stretch
2889	C—H stretch
1467	CH_2 asymmetric deformation; CH_2 scissor vibration
1360	CH_2 wag; C—O stretch
1280, 1114, 1060	C—O—C vibrations
947	C—H out-of-plane bending
842	C—C stretch

amounts of NIPA and AMPS to give 10.0 mmol of the monomers in 11.3 mL of deionized water, together with 0.17 mmol of PEG6000, 0.05 mmol of APS, and 0.35 mmol of MBAA. A 1.6-mL aliquot of each pregel solution was transferred to a polytetrafluoroethylene (PTFE) cylindrical vessel with an internal diameter of 26 mm. The vessels were closed with PTFE lids and heated at 70°C in a water bath at 70°C for 2 h. The resulting gels were vacuum-dried at 70°C.

Fourier transform infrared (FTIR) spectra of PEG, NIPA, and AMPS homopolymers, NIPA/AMPS copolymers, and dried SIPNs incorporated into KBr discs were obtained with a Bio-Rad model FTS-60 spectrophotometer (Hercules, CA).

X-ray photoelectron spectroscopy (XPS) was carried out with a Kratos model XSAM 800 instrument (Manchester, UK) with an Al Kα (1486.6 eV) X-ray source at 10 kV, 40 mA , and 3×10^{-9} Torr on dried gel powders pressed into pellets. The observed binding energies were charge-corrected to the saturated hydrocarbon peak (C1s = 285.0 eV).

Differential scanning calorimetry (DSC) scans were recorded with a Polymer Laboratories model 12000 instrument (Church Stretton, UK) with two to four repeated determinations at a scanning rate of 10°C/min. The samples were encapsulated in an aluminum pan and heated and cooled in an atmosphere of flowing dry nitrogen.

The crystallinity of the dried samples was examined by X-ray powder diffraction with a Philips PW1130 diffractometer (Eindhoven, The Netherlands).

A Philips XL30 scanning electron microscope was used to investigate the surface morphology of the dried gels.

RESULTS AND DISCUSSION

FTIR spectroscopy

FTIR spectral data for PEG6000, poly(2-acrylamido-2-methylpropanesulfonic acid) (polyAMPS), poly(*N*-isopropylacrylamide) (polyNIPA), and dried poly(AMPS-*co*-NIPA) copolymer gels and PEG/poly(AMPS-*co*-NIPA) SIPNs are shown in Tables I–III.

The PEG6000 spectrum is virtually identical to the reference spectrum for PEG3400.

TABLE II
FTIR Spectra of AMPS and NIPA Homopolymers and Poly(AMPS-*co*-NIPA) Copolymer Gels

Sample	ν for the major bands (cm^{-1})	R_I[a]
PolyAMPS	3469, 3326, 3120, 2945, 1651, 1557, 1372, 1225, 1180, 1039, 623	1.61
0.60 AMPS/0.40 NIPA copolymer gel	3436, 3308, 3085, 2980, 2936, 1651, 1556, 1462, 1392, 1370, 1224, 1179, 1039, 623	1.09
0.50 AMPS/0.50 NIPA copolymer gel	As above for the 0.60 AMPS/0.40 NIPA gel, except for insignificant band shifts and relative intensity variations	0.99
PolyNIPA	3435, 3294, 3080, 2974, 2932, 1652, 1557, 1457, 1172	0

[a] Intensity ratio of the 1038 ± 2 cm^{-1} band to the 1650 ± 2 cm^{-1} band.

For the polyAMPS, polyNIPA, and poly(AMPS-*co*-NIPA) copolymers, the spectral assignments of the principal bands of interest are as follows:[27–29]

3500–3200 cm^{-1} : N—H stretch from amide groups of AMPS and NIPA and overlapping O—H stretch from the sulfonic acid group in AMPS.
1652 cm^{-1} : secondary amide carbonyl groups in AMPS and NIPA.
1552–1557 cm^{-1} : secondary amide N—H deformation in the solid state.
1039 cm^{-1} : SO_3 symmetric stretch (AMPS).
1224–1225 cm^{-1} : SO_2 asymmetric stretch (AMPS).
623–624 cm^{-1} : C—S stretch (AMPS).

The C—N stretch band is at 1180 cm^{-1} for polyAMPS, at 1172 cm^{-1} for polyNIPA, and at 1178–1179 cm^{-1} for the AMPS—NIPA copolymers. There is no olefinic band ($\nu_{C=C}$) at 1635–1620 cm^{-1}, and this indicates the complete conversion of the monomers. The NH vibrational bands occur in the 3435–3469-cm^{-1} range. The

TABLE III
Comparison of FTIR Spectra for PEG/Poly(AMPS-*co*-NIPA) SIPNs with Various Proportions of AMPS and NIPA

SIPN	ν for the major bands (cm^{-1})	R_I[b]
PEG/polyAMPS	3308, 2922, 1652, 1558, 1456, 1353, 1228, 1108, 1039, 953, 948, 624	2.52
PEG/poly (AMPS-*co*-NIPA)[a]	3309, 3084, 2975, 2933, 1658, 1651, 1553, 1462, 1369, 1352, 1228, 1179, 1112, 1039, 950, 844, 624	1.48
PEG/polyNIPA	3433, 3306, 3073 2971, 2933, 1655, 1648, 1545, 1459, 1387, 1367, 1274, 1172, 1130, 839	0

[a] NIPA/AMPS comonomer ratio = 1 : 1.
[b] Intensity ratio of the 1038 ± 2 cm^{-1} band to the 1650 ± 2 cm^{-1} band.

TABLE IV
Thermal Properties of PEG6000

Transition	Temperature (°C)	ΔH (J/g)
Glass transition (T_g)	−41	—
Melting onset (T_m)	59	256 ± 43
Melting peak (T_{mp})	64	
Recrystallization onset (T_r)	43	230 ± 5
Recrystallization peak (T_{rp})	38	
Decomposition onset (T_d)	372	233 ± 17
Decomposition peak (T_{dp})	393	

The data are mean values derived from multiple DSC scans.

ΔH is the associated enthalpy change.

intensity ratio (see Table II) decreases with an increasing proportion of AMPS because the intensity of the 1652 ± 2 cm^{-1} band is proportional to the total amount of carbonyl from the amide groups.

The FTIR spectra of the SIPNs (Table III) are significantly different in some respects from the spectra of the corresponding poly(AMPS-*co*-NIPA) copolymers (Table II), PEG (Table I), and NIPA and AMPS homopolymers (Table II). The weak O—H stretch at 3448 cm^{-1} in PEG corresponds to a much stronger band (OH and NH stretch) at 3433 cm^{-1} in the PEG/polyNIPA SIPN. Other features of the SIPN spectra are bands at 3306 (N—H stretch) and 3073 cm^{-1} (C—H stretch from the —O—CH_2CH_2— units), the quite strong 2971-cm^{-1} band [CH_3 asymmetric stretch from $N(CH_3)$], the band at 2933 cm^{-1} (CH_2 asymmetric stretch), and C—N stretch at 1172–1179 cm^{-1}. The bands at 1108 cm^{-1} in the PEG/polyAMPS SIPN, at 1112 cm^{-1} in the PEG/50 mol % AMPS SIPN, at 1130 cm^{-1} in the PEG/polyNIPA SIPN, and at 1114 cm^{-1} in PEG6000 are associated with the C—O stretch of the ethylene glycol unit.[30] In polyAMPS and the SIPN with 50% AMPS, the strong 3308–3309-cm^{-1} bands are attributed to the O—H vibration and (N—H···O) hydrogen bonds. The broad band at 3500–3300 cm^{-1} in the copolymer gel becomes narrower in the same region in the SIPN. The 3337-cm^{-1} band of the copolymer gel is shifted to 3309 cm^{-1} in the SIPN gel, possibly because of the interaction between PEG and poly(AMPS-*co*-NIPA) networks, in which more intermolecular hydrogen bonds form between oxygen atoms in PEG chains and N—H groups in copolymer chains.

Thermal analysis

Data from the DSC scans are given in Tables IV and V. A mechanistic study[31] has shown that at temperatures above 190°C, polyacrylamide or poly(*N*-alkyl-substituted acrylamide) will generate cyclic imide or nitrile groups with RNH_2, RNHR, or ROH. This temperature range is close to our observation of an initial decomposition at ~223°C (Table V) for polyNIPA. A thermogravimetric analysis/FTIR study indicated[32] that the NIPA homopolymer degraded with almost no residue, mainly at about 400°C, which is close to the fourth decomposition peak that we have observed (at 406°C) for polyNIPA.

The glass-transition temperature found for polyAMPS is close to the value (123 ± 1°C) observed for a polyAMPS gel made by irradiation,[33] a lower glass-transition temperature being expected for the noncrosslinked polymer. The first clearly defined decomposition temperature for the irradiated and dried AMPS homopolymer gel was found at about 170°C,[33] in reasonable accordance with the value (180°C) for the free-radical-initiated homopolymer. The free-radical-initiated AMPS homopolymer shows a second decomposition peak at 190°C and a third at 311°C that is attributed to main-chain scission at a temperature close to that (303°C) found for the principal decomposition of the AMPS homopolymer gel made by irradiation.[33]

DSC data for the poly(AMPS-*co*-NIPA) gel with equimolar proportions of AMPS and NIPA and one SIPN with 95 mol % NIPA and 10 wt % PEG are shown in Table V. The principal decomposition, attributed to main-chain scission, was found at 312°C. The first decomposition temperatures for the SIPNs (the data for one of them are given in Table V) were virtually independent of the crosslinker concentration and significantly higher than those for the corresponding copolymer gels. In addition, the SIPNs undergo thermal decomposition in two stages rather than the three stages observed for the copolymer gels. These observations suggest the existence of relatively strong interactions between ether oxygens in the PEG chains and hydrogen-bond donors in the copolymer chains that enhance the thermal stability of the copolymer network.

TABLE V
Thermal Properties of PolyNIPA, PolyAMPS, Poly(AMPS-*co*-NIPA), and PEG/Poly(AMPS-*co*-NIPA) SIPNs

Sample	T_g (°C)[a]	$T_{d,1}$ (°C)[b]	$T_{d,2}$ (°C)[b]	$T_{d,3}$ (°C)[b]	$T_{d,4}$ (°C)[b]
PolyNIPA	136 ± 4	223	286	348	406
PolyAMPS	115 ± 5	180	190	311	—
Poly(AMPS-*co*-NIPA)[c]	123 ± 4	203	—	312	407
PEG/poly(AMPS-*co*-NIPA) SIPN[d]	—	289	415	—	—

[a] Glass transition temperature.

[b] Decomposition temperature, evaluated as the peak temperature of exothermic transition.

[c] Dried gel, from reaction mixture with comonomer ratio 1 : 1.

[d] Dried SIPN gel, from reaction mixture with 10 wt % PEG, 5 mol % AMPS and 95 mol % NIPA, and 4.2 wt % MBAA.

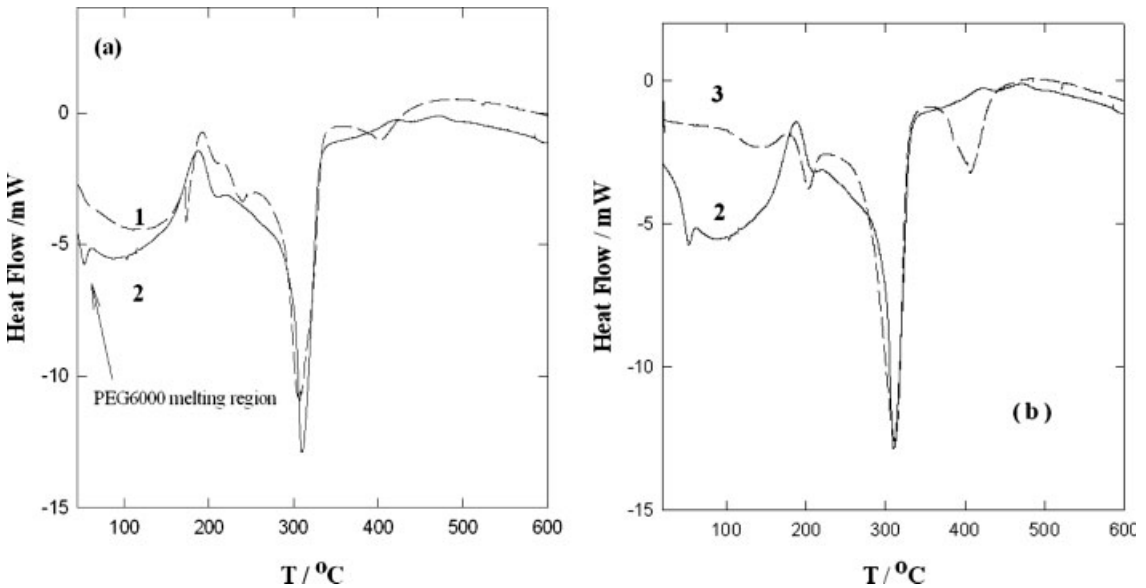

Figure 1 DSC scans: (a) thermal behavior of PEG/poly(AMPS-*co*-NIPA) SIPNs with (1) 10 or (2) 41.8 wt % PEG and (b) comparison of SIPNs with copolymer gels. Curve 2 is the same as the curve in part a. Curve 3 refers to the poly(AMPS-*co*-NIPA) copolymer gel with equimolar proportions of AMPS and NIPA.

It was anticipated that PEG6000 dispersed in the copolymer network in the course of copolymerization and crosslinking would exhibit its characteristic behavior when its concentration was sufficient to form a PEG6000 microphase or domain in the SIPN. However, it is feasible that behavior characteristic of PEG at a lower concentration in the SIPN system could be inhibited by interactions such as hydrogen bonds between PEG and the AMPS–NIPA network. To elucidate these points, thermal analyses were carried out on SIPNs with various PEG6000 contents. Figure 1(a) shows that for the SIPN with 41.8% PEG6000, there was a repeatable, small endotherm in the vicinity of 53–59°C whose area varied somewhat with the thermal history of the sample. This endotherm was attributed to the melting of the PEG6000 microphase in the SIPN. Pure PEG6000 was found to melt at a temperature in the range of 62–65°C, which is 6–9°C higher than the range of the melting temperatures for PEG in the SIPN. For a macromolecular two-component system in which both components have a large molar mass, the two-phase, two-component melting-point-lowering effect can be expressed by[34]

$$\frac{1}{T_m} - \frac{1}{T_m^o} = -\frac{RV_{2u}}{\Delta H_{2u} V_{1u}} \chi (1 - \phi_2)^2 \qquad (1)$$

where component 2 is the crystallizing macromolecule and 1 is the macromolecular diluent. T_m is the melting temperature, and T_m^o is the melting temperature in the absence of diluent, and R is the gas constant. V_{1u}, V_{2u}, ΔH_{2u}, χ, and ϕ_2 are the repeat unit molar volumes of components 1 and 2, the repeat unit molar enthalpy of fusion for component 2, the interaction parameter, and the volume fraction of component 2, respectively. Equation (1) indicates that sizeable melting-point lowering is expected only in a system with a negative value of the Flory–Huggins parameter, χ.[35–37] Specific effects such as interactions between donor–acceptor groups, the match of steric configurations of the components, the orientation of polar bonds, and hydrogen bonding may lead to a negative heat of mixing and enhance solubility. For PEG6000 as component 2 and

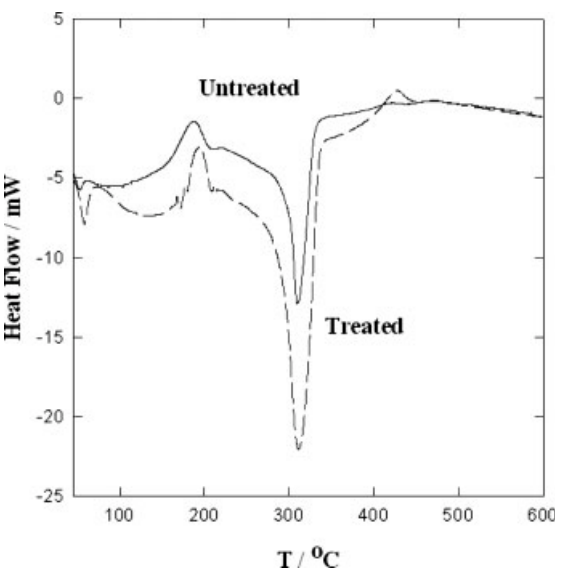

Figure 2 Thermal behavior of (- - -) heat-treated and (—) untreated 41.8 wt % PEG SIPN gels with 50 mol % AMPS. *Heat-treated* refers to a sample that was held at 80°C for 10 min and then cooled and reheated; *untreated* refers to a sample of the same material that was not subjected to heat treatment before the DSC scan.

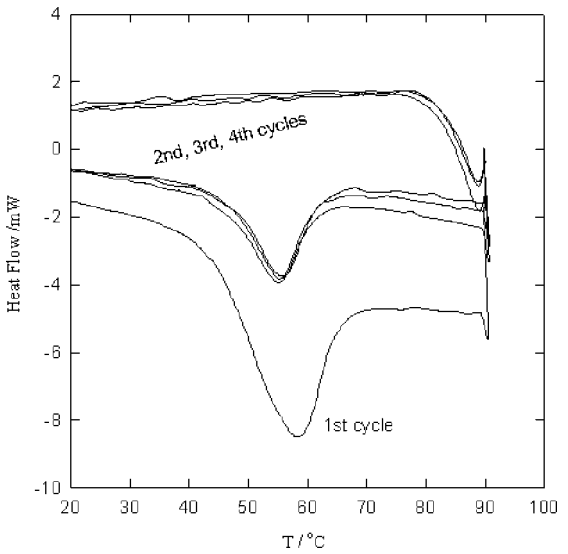

Figure 3 Multicyclic DSC scans for an SIPN with 41.8 wt % PEG that was heated and cooled at 10°C/min between −20 and 90°C.

the copolymer network as the other component, the lowering of the melting point of PEG6000 in the SIPN provides additional evidence for relatively strong interactions between PEG6000 and the copolymer network, the noncrystalline polymer acting as a diluent that reduces the melting temperature of the crystalline phase.

The lowering of the melting point of a semicrystalline polymer in a blend has been taken as evidence of some degree of miscibility in the amorphous phases.[38] Another possible explanation for the melting-point depression is decreased crystal size of PEG6000 through the formation of a microphase of PEG6000. In the *in situ* copolymerization/blending processes, there is a mixture of morphological units, crystal imperfections, and overwhelming surface from microphases in the SIPN systems. The smaller microcrystals and larger surface areas cause the subsystem of PEG6000 in the SIPN to increase its internal energy. The large surface area of the small crystals increases the free energy of the average crystalline subsystem above the free energy of the equilibrium crystal, leading to the melting-point depression.

TABLE VI
XPS Data from the Survey Scan

Corrected	O1s (1)	N1s (1)	C1s (1)	S2p (1)
BE (eV)[a]	532.85	399.85	285.85	167.85
fwhm (eV)[b]	2.70	2.62	3.26	3.03
Raw area	124258	9622	114836	4287
Atomic concentration (%)	27.75	3.38	67.70	1.17

[a] Binding energy calibrated with C in saturated hydrocarbon (C1s = 285.0 eV).
[b] Full width at half-maximum.

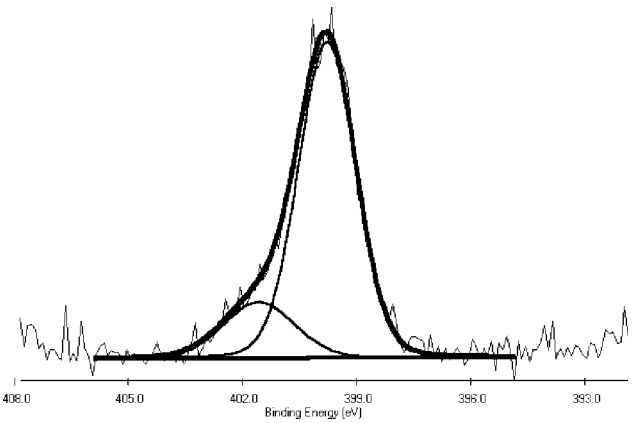

Figure 4 Typical XPS spectrum for N1s.

That the melting endotherms and melting points are also influenced by the proportion of PEG is indicated by the DSC scans in Figure 1. Figure 1(a) shows that reducing the proportion of PEG6000 in the SIPN from 41.8 (curve 2) to 10 wt % (curve 1) changes the thermal behavior such that the melting endotherm at about 58°C in the 41.8% PEG SIPN is not detected in that temperature region for the SIPN with 10 wt % PEG. Figure 1(b) compares the thermal behavior of the SIPN (curve 2) with that of the copolymer (curve 3) gel with corresponding proportions of the comonomers. It is evident that the principal decomposition for the SIPN gels is determined by the copolymer network, as expected. The SIPN with a low (10 wt %) PEG content [Fig. 1(a), curve 1] behaves more like the copolymer [Fig. 1(b), curve 3] than the SIPN with 41.8% PEG.

Figure 2 shows that the enthalpy of fusion for PEG in the SIPN with 41.8% PEG increased after the sample was held for 10 min at 80°C. The increase is attributable to increased PEG microphase separation and subsequent crystallization of those domains. An increase in the enthalpy change for the principal decomposi-

TABLE VII
Subband Assignments

Element	Binding Energy (eV)	Assignment
C1s	285.0	Aliphatic C, CH_x, C—C, C—SO_3
	286.6	C—O, C—O—C, C—N
	288.1	C=O
O1s	532.9	Aliphatic O, C=O, C—O—C, C—OH, bound water O—H
	531.1	O=C—N, —SO_2— or —SO_3^-
S2p	168.3	—SO_3^-
	169.6	$S_2O_8^{2-}$ from the APS initiator
N1s	399.8	—CONH
	401.6	—$CONH_2^+$

The assignments are taken from refs. 39–43. The scan resolution was 0.1 eV.

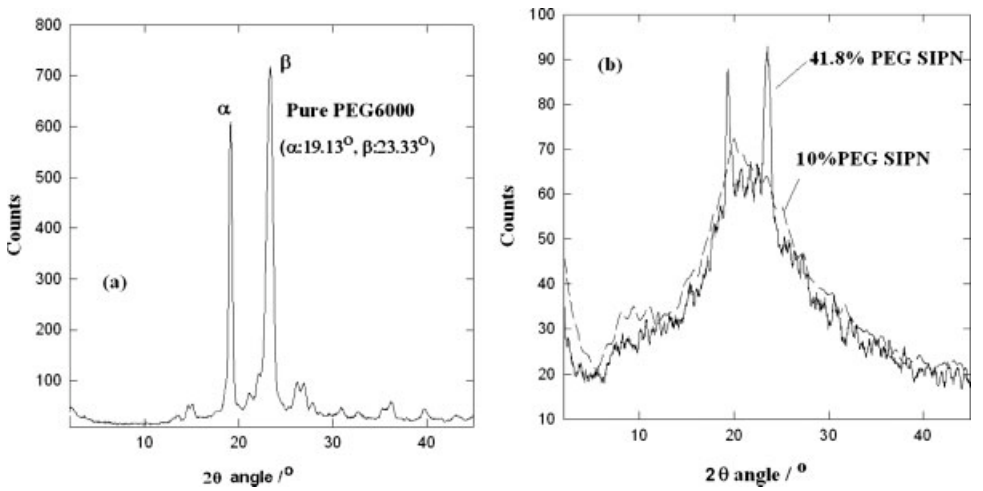

Figure 5 Wide-angle X-ray diffraction spectra for (a) a PEG6000 powder and (b) SIPNs with 41.8 wt % PEG (shown by a solid line) and 10 wt % PEG (shown by a broken line).

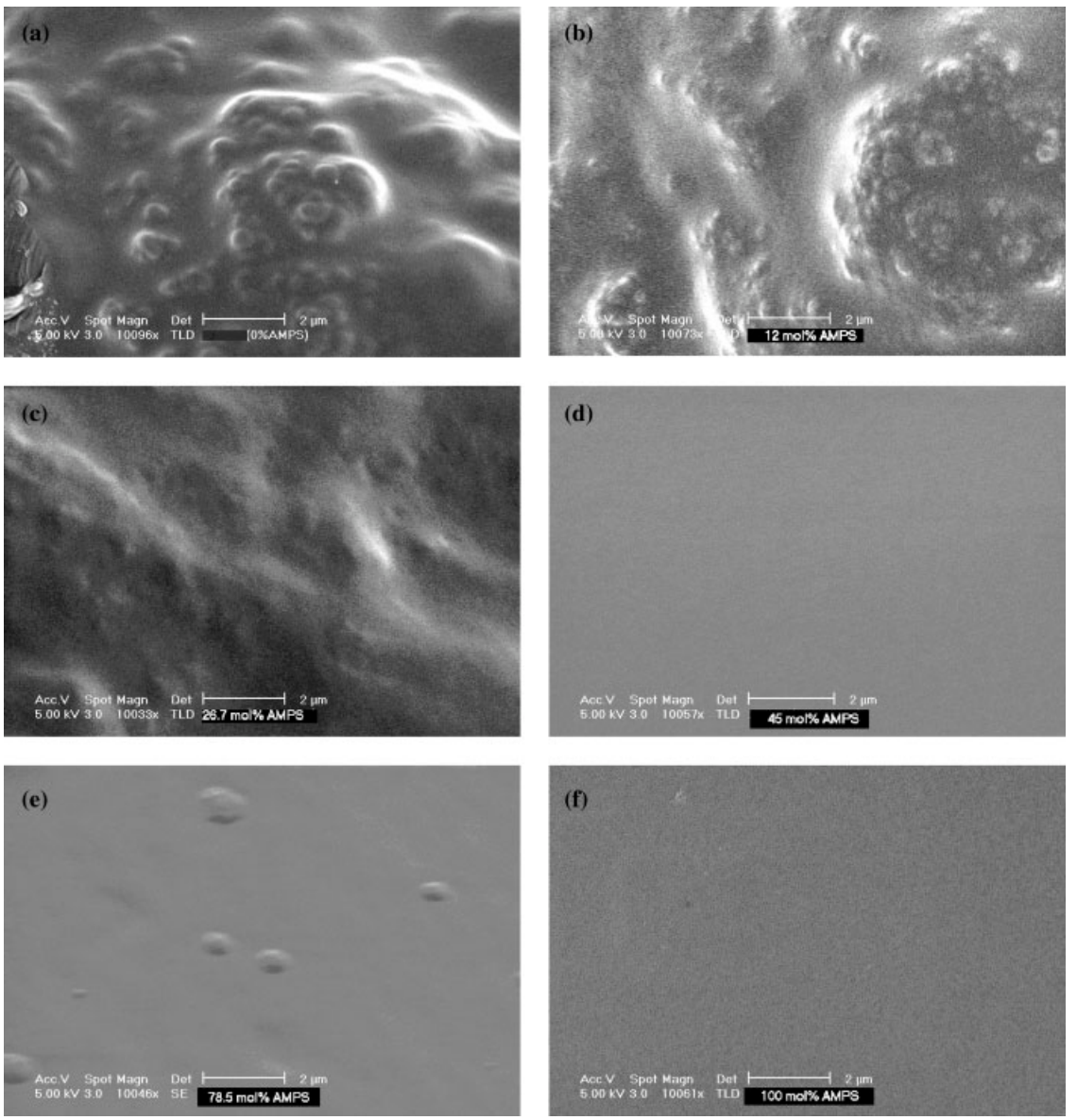

Figure 6 Scanning electron micrographs of AMPS–NIPA copolymers: (a) 0, (b) 12, (c) 26.7, (d) 45, (e) 78.5, and (f) 100 mol % AMPS.

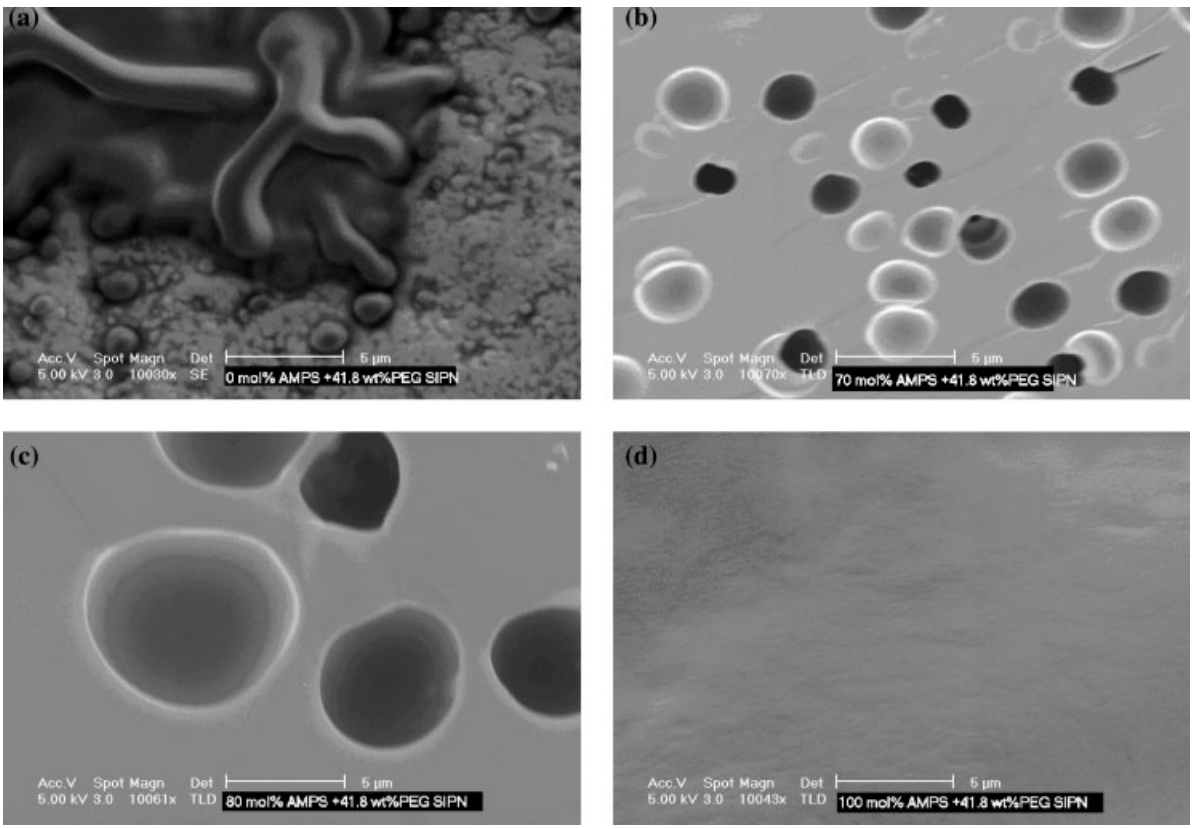

Figure 7 Scanning electron micrographs (from the surface) of PEG/poly(AMPS-*co*-NIPA) SIPNs: (a) 0, (b) 70, (c) 80, and (d) 100 mol % AMPS.

tion, after the heat treatment, was also found. It appears that increased PEG microphase separation facilitates the changes that occur at the first decomposition temperature, but in the absence of information on the nature of the decomposition reaction, it is difficult to be more specific about the role of PEG in that process. The other significant changes above 100°C for both SIPNs in Figure 2 might possibly come from segmental movements of PEG and/or release of internal stress.

Figure 3 shows the effects of the thermal history (recycling between the same temperature limits) on the thermal properties of the SIPN with 41.8% PEG. The melting endotherm at 58°C in the untreated 41.8 wt % PEG sample was reproduced at a temperature about 3°C lower (with minor variations) in subsequent cycles, whereas the associated enthalpy change decreased by about 60% after the first heating scan. The large reduction in the enthalpy of fusion is attributed to a loss of residual water in the first heating scan.

XPS analysis

A dried SIPN powder with 41.8 wt % PEG and a 4 : 6 molar ratio of AMPS to NIPA was pressed into a pellet for XPS analysis. Atomic concentrations derived from a survey scan are given in Table VI. Subband analyses were carried out with the software package XPSPEAK (version 4.1) assuming a 10% Gaussian–Lorentzian band profile. The subband analysis for N1s is shown in Figure 4, and the subband assignments for O1s, N1s, C1s, and S2p are given in Table VII. It was found that 18% of the N is in the form of $—CONH_2^+$, which arises from protonation of —CONH groups by the sulfonic acid groups. The basis for that conclusion is the positive shift in the binding energy together with the higher oxidation state.[39]

The swelling behavior of poly(NIPA-*co*-AMPS) hydrogels in aqueous solutions of PEG300 and PEG400 has been reported.[26] It was concluded that attractive interactions between PEG and NIPA segments were responsible for the re-entrant phase observed for gels containing 1.0 mol % neutralized AMPS segments. However, swollen gels with more than 3 mol % neutralized AMPS remained in the swollen state over all PEG volume fractions because the osmotic pressure of counterions inside the gel increased the gel volume, so the PEG chains could easily penetrate the poly(NIPA) network without an essential loss of their conformational entropy and could interact with water inside the gel phase. In our dried SIPNs, for which DSC scans are shown in Figure 1, hydrophobic interactions between isopropyl groups in NIPA segments and ethylene groups (CH_2CH_2) in PEG and the osmotic pressure of

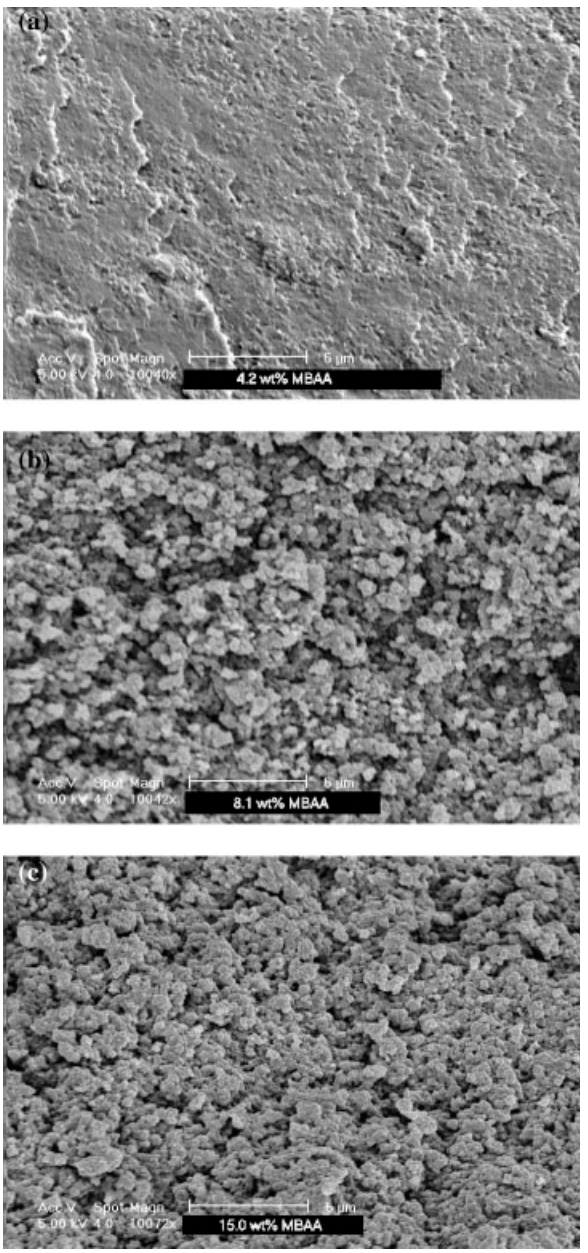

Figure 8 Effect of the MBAA concentration on the cross-section morphology of dried SIPNs (with 5 mol % AMPS, 95 mol % NIPA, and 10 wt % PEG): (a) 4.2, (b) 8.1, and (c) 15.0 wt % MBAA.

counterions should be quite strong, together with hydrogen bonding between ether oxygens of PEG chains and hydrogen atoms of $—CONH_2^+$ groups in the copolymer chains.

X-ray diffraction (XRD)

XRD patterns for pure PEG6000 and SIPNs with 41.8 and 10 wt % SIPN, in a dry powder form, are shown in Figure 5. Pure PEG6000 [Fig. 5(a)] has strong Bragg reflections at 2θ values of 19.13 and 23.33°. Those reflections were found with much smaller intensity in the SIPN with 41.8 wt % PEG at 19.40 and 23.51° [Fig. 5(b)]. It appears that during dehydration of the hydrogel with the higher proportion of PEG, the PEG6000 molecules had sufficient mobility to form a PEG-rich region, in which a crystalline microphase was able to be formed. In the sample with 10 wt % PEG, the characteristic PEG reflections were not observed, and this indicated that in that SIPN virtually all the PEG molecules were involved in sufficiently strong interactions with the copolymer network to prevent the formation of a crystalline PEG microphase.

Morphology

The scanning electron micrographs in Figure 6 show that the surface morphology of dried AMPS–NIPA copolymer gels changes markedly with the copolymer composition. A comparison of Figure 7 with Figure 6 reveals that PEG6000 changes the morphology of the samples after vacuum drying, and increasing the AMPS content in the copolymer gels and SIPNs decreases the surface roughness. The cavities that appear in the surfaces of some SIPNs can be attributed to water loss during the vacuum drying of the materials at 70°C. It appears that the ability of the gels to retain water may be enhanced by the presence of both AMPS and PEG in the gels, except for the SIPN with zero NIPA content [Fig. 7(d)]. The rootlike structures revealed in Figure 7(a) might be formed as the result of interfacial tension of NIPA-rich domains, while the temperature was above the LCST of NIPA units, at a relatively low crosslinker concentration.

Scanning electron micrographs (Fig. 8) of dried SIPN gels with various MBAA concentrations show a striking morphological change at crosslinker concentrations above about 4 wt %. The essentially continuous single phase becomes increasingly fragmented, with an average fragment size of approximately 200 nm. The nanogels obviously have a very large specific surface area and should swell much more rapidly in aqueous media than gels with a continuous phase structure. The unique properties of PEG/poly(AMPS-*co*-NIPA) SIPNs, which have pH and thermal responsiveness and releasable PEG molecules, have been used in the development of a drug encapsulation/delivery system, which will be reported elsewhere.

CONCLUSIONS

Although the properties of SIPNs are determined primarily by the copolymer chain composition, the presence of PEG in these materials enhances their thermal stability versus that of copolymer gels with corresponding comonomer compositions and influences the morphology of the gels. Strong hydrophobic and hydrogen-bonding interactions between PEG molecules and functional groups on the copolymer chains

are most likely the basis of these effects and limit the formation of a crystalline PEG microphase to gels that have a high proportion (ca. 40 wt %) of PEG.

The authors thank Yan Jin, Peter Buchanan, Ritchie Sims, and Catherine Hobbis for their invaluable assistance with the instrumental analyses.

References

1. Heskins, M.; Guillet, J. E. J Macromol Sci Chem 1968, 2, 1441.
2. Yoshida, R.; Uchida, K.; Kaneko, Y.; Sakai, K.; Kikuchi, A.; Sakurai, Y.; Okano, T. Nature 1995, 374, 240.
3. Priest, J. H.; Murray, S. L.; Nelson, R. J.; Hoffman, A. S. In Reversible Polymeric Gels and Related Systems; Russo, P. S., Ed.; American Chemical Society: Washington, DC, 1987; Chapter 18, p 255.
4. Mumick, P. S.; McCormick, C. L. Polym Eng Sci 1994, 34, 1419.
5. Kaneko, Y.; Sakai, K.; Kikuchi, A.; Yoshida, R.; Sakurai, Y.; Okano, T. Macromolecules 1995, 28, 7712.
6. Yoo, M. K.; Sung, Y. K.; Lee, Y. M.; Cho, C. S. Polymer 1998, 39, 3703.
7. Travas-Sejdic, J.; Easteal, A. J. Polymer 2000, 41, 7451.
8. La Combe, E. M.; Miller, W. P. U.S. Patent 3,332,904 (1967).
9. Killam, H. S. U.S. Patent 3,544,597 (1970).
10. Helling, G.; Krafft, W.; Findeisen, K.; Himmelmann, W. Ger. Patent 2,911,694 (1980).
11. Taylor, L. D.; Sullivan, C. I.; Bedell, S. F. Ger. Patent 2,910,270 (1980).
12. Wright, P. J. Eur. Patent 15,879 (1980).
13. Polaroid Corp. Jpn. Pat. JP 55041490 (1980).
14. Anonymous Res Discl 1980, 191, 126.
15. Walworth, V. K.; Gerber, A. M. Ger. Patent 2,714,489 (1977).
16. Priest, W. J. Res Discl 1977, 159, 7.
17. Weber, W. W., II; Heseltine, D. W. U.S. Patent 4,045,229 (1977).
18. Chen, T. J.; Abel, E. P. Res Discl 1977, 161, 48.
19. Tsuji, N.; Yamaguchi, J. Jpn. Patent 5,1130,217 (1976).
20. Tsuji, N. Jpn. Patent 5,1061,823 (1976).
21. Brandt, K. A.; Goldman, S. A.; Inglin, T. A. Eur. Patent 205,674 (1986).
22. Ito, K.; Shibano, T. Patent 63,260,906 (1988).
23. Zhang, C.; Easteal, A. J. J Appl Polym Sci 2003, 88, 2563.
24. Zhang, C.; Easteal, A. J. J Appl Polym Sci 2004, 91, 3635.
25. Zhang, C.; Easteal, A. J. J Appl Polym Sci 2004, 94, 2083.
26. Melekaslan, D.; Okay, O. Macromol Chem Phys 2001, 202, 304.
27. Socrates, G. Infrared Characteristic Group Frequencies: Tables and Charts, 2nd ed.; Wiley: Chichester, England, 1994; p 249.
28. Every, H.; Forsyth, M.; MacFarlane, D. R. Ionics 1996, 2, 53.
29. Aggour, Y. A. Polym Degrad Stab 1994, 45, 273.
30. Shojaei, A. H.; Li, X. J Controlled Release 1997, 47, 151.
31. Bae, S. S.; Chakrabarty, K.; Seery, T. A. P.; Weiss, R. A. J Macromol Sci Pure Appl Chem 1999, 36, 931.
32. Schild, H. G. J Polym Sci Part A: Polym Chem 1996, 34, 2259.
33. Zhang, C.; Easteal, A. J. J Appl Polym Sci 2003, 89, 1322.
34. Wunderlich, B. In Thermal Characterization of Polymeric Materials; Turi, E. A., Ed.; Academic: San Diego, 1997; Vol. 1, p 205.
35. Flory, P. J. J Chem Phys 1941, 9, 660.
36. Huggins, M. L. J Chem Phys 1941, 9, 440.
37. Muthukumar, M.; Edwards, S. F. In Comprehensive Polymer Science: The Synthesis, Characterization, Reactions & Applications of Polymers; Allen, G.; Bevington, J. C., Eds.; Pergamon: Oxford, 1989; Vol. 2, p 1.
38. Hale, A.; Bair, H. E. In Thermal Characterization of Polymeric Materials; Turi, A., Ed.; Academic: San Diego, 1997; Vol. 1, p 745.
39. Nefedov, V. I. X-Ray Photoelectron Spectroscopy of Solid Surfaces, 1st ed.; VSP: Utrecht, The Netherlands, 1988; p 191.
40. Eberhart, J. P. Structural and Chemical Analysis of Materials; Wiley: Chichester, England, 1991; p 333.
41. Moulder, J. F.; Stickle, W. F.; Sobol, P. E.; Bomben, K. D. Handbook of X-Ray Photoelectron Spectroscopy: A Reference Book of Standard Spectra for Identification and Interpretation of XPS Data; PerkinElmer: Eden Prairie, MN, 1992.
42. Buchman, A.; Dodiuk, H.; Rotel, M.; Zahavi, J. In Polymer Surfaces and Interfaces: Characterization, Modification and Application; Mittal, K. L.; Lee, K.-W., Eds.; VSP: Utrecht, The Netherlands, 1997; p 37.
43. Beamson, G.; Briggs, D. High Resolution XPS of Organic Polymers: The Scienta ESCA300 Database; Wiley: Chichester, England, 1992; p 295.